




Article

Sensing the Environmental Inequality of PM_{2.5} Exposure Using Fine-Scale Measurements of Social Strata and Citizenship Identity

Li He ^{1,†} , Lingfeng He ^{1,*,†} , Zezheng Lin ² , Yao Lu ³, Chen Chen ⁴, Zhongmin Wang ⁵, Ping An ⁶, Min Liu ⁶, Jie Xu ⁷ and Shurui Gao ¹

¹ Institute for Empirical Social Science Research, School of Humanities and Social Science, Xi'an Jiaotong University, Xi'an 710049, China; lihegeo@xjtu.edu.cn (L.H.); gaoshurui@stu.xjtu.edu.cn (S.G.)

² Steering Committee of ESG & Carbon Neutral Investment, United Nations Industrial Development Organization, Beijing 100060, China; jasonlinzezheng@gmail.com

³ Rackham Graduate School, University of Michigan, Ann Arbor, MI 48109, USA

⁴ Xi'an Jiaotong University Press, Xi'an 710049, China

⁵ Xi'an Public Security Bureau, Xi'an 710002, China

⁶ School of Management, Xi'an Jiaotong University, Xi'an 710049, China; anping@stu.xjtu.edu.cn (P.A.); liumin0@stu.xjtu.edu.cn (M.L.)

⁷ School of Economics and Finance, Xi'an Jiaotong University, Xi'an 710049, China

* Correspondence: helingfeng@stu.xjtu.edu.cn

† These authors contributed equally to this work.

Abstract: Exposure to PM_{2.5} pollution poses substantial health risks, with the precise quantification of exposure being fundamental to understanding the environmental inequalities therein. However, the absence of high-resolution spatiotemporal ambient population data, coupled with an insufficiency of attribute data, impedes a comprehension of the environmental inequality of exposure risks at a fine scale. Within the purview of a conceptual framework that interlinks social strata and citizenship identity with environmental inequality, this study examines the environmental inequality of PM_{2.5} exposure with a focus on the city of Xi'an. Quantitative metrics of the social strata and citizenship identities of the ambient population are derived from housing price data and mobile phone big data. The fine-scale estimation of PM_{2.5} concentrations is predicated on the kriging interpolation method and refined by leveraging an advanced dataset. Employing geographically weighted regression models, we examine the environmental inequality pattern at a fine spatial scale. The key findings are threefold: (1) the manifestation of environmental inequality in PM_{2.5} exposure is pronounced among individuals of varying social strata and citizenship identities within our study area, Xi'an; (2) nonlocal residents situated in the northwestern precincts of Xi'an are subject to the most pronounced PM_{2.5} exposure; and (3) an elevated socioeconomic status is identified as an attenuating factor, capable of averting the deleterious impacts of PM_{2.5} exposure among nonlocal residents. These findings proffer substantial practical implications for the orchestration of air pollution mitigation strategies and urban planning initiatives. They suggest that addressing the wellbeing of the marginalized underprivileged cohorts, who are environmentally and politically segregated under the extant urban planning policies in China, is of critical importance.

Keywords: PM_{2.5} exposure; environmental inequality; social stratum; citizenship identity; spatial analysis



Citation: He, L.; He, L.; Lin, Z.; Lu, Y.; Chen, C.; Wang, Z.; An, P.; Liu, M.; Xu, J.; Gao, S. Sensing the Environmental Inequality of PM_{2.5} Exposure Using Fine-Scale Measurements of Social Strata and Citizenship Identity. *ISPRS Int. J. Geo-Inf.* **2024**, *13*, 257. <https://doi.org/10.3390/ijgi13070257>

Academic Editors: Wolfgang Kainz, Lan Mu and Jue Yang

Received: 14 May 2024

Revised: 7 July 2024

Accepted: 15 July 2024

Published: 17 July 2024



Copyright: © 2024 by the authors. Licensee MDPI, Basel, Switzerland. This article is an open access article distributed under the terms and conditions of the Creative Commons Attribution (CC BY) license (<https://creativecommons.org/licenses/by/4.0/>).

1. Introduction

Air pollution exposure is recognized as a complex and multifaceted challenge that intersects the disciplines of geography, public health, environmental science, and the social sciences. The exposure to air pollutants, both short-term and long-term, whether acute or chronic, has been consistently associated with an array of adverse health outcomes,

including an elevated risk of cardiopulmonary and respiratory diseases [1–4], as well as increased mortality rates [1,5,6]. Moreover, emerging evidence suggests that air pollution may induce cognitive decline [7] and depressive disorder [8]. A substantial body of research has demonstrated that the health risks associated with air pollution are not evenly distributed across the population, with disparities often linked to socioeconomic status and ethnicity, a phenomenon that reflects the spatial distribution of pollution and is encapsulated by the concept of environmental inequality [9,10].

Environmental inequality has risen as a critical issue in air pollution exposure research [10]. A substantial body of research has furnished compelling evidence highlighting the disproportionate impact on vulnerable populations characterized by low socioeconomic status, including limited education, low occupational status, unemployment, and poverty [11,12]. Additionally, the lack of housing ownership [13,14] and racial or ethnic-based social exclusion, particularly affecting Black, Latinx, and Indigenous communities [15–17], have been identified as significant factors contributing to disparities in air pollution exposure and the ensuing health consequences. These patterns of disparity have been extensively studied from the 1970s to the present, transcending geographical boundaries and manifesting in both urban and rural settings [12,14,16,18], across developing and developed nations [12,16,19,20], and even in societies considered to be more egalitarian [21].

In recent years, fruitful advancements have been made in understanding environmental inequality in air pollution exposure in China [10,22]. However, the reliance on static population data sourced from censuses and yearbooks at the administrative division level presents limitations, as it does not account for the dynamic nature of human activities and the daily spatial distribution of the ambient population [23–25]. It is important to recognize two key limitations when working with static data such as census records. First, residents' daily activities are not confined by the boundaries of blocks, census tracts, or administrative districts. Analyzing spatial patterns using a regular grid as the unit of assessment, instead of administrative divisions, mitigates the issue of arbitrarily assigning demographic and socioeconomic indicators based on artificial boundaries, further ensuring the validity of pollution exposure assessments. Second, static data such as census population data fail to account for residents' characteristics of travel activities, making it uncondusive to accurately depicting the daily average spatial distribution of the population.

To address these limitations, there has been a shift towards utilizing high-resolution global population data represented through regular grids, such as footfall data [26], LandScan [27,28], and WorldPop [29]. These data offer enhanced spatial resolution, but are limited by the absence of attribute data that characterize the ambient population (i.e., spatiotemporally dynamic population) [30]. This ongoing gap constrains scholars' capacity to fully comprehend the risks associated with pollution exposure and environmental equality at the fine scale.

Advancements in data collection technology present an opportune avenue for overcoming the aforementioned challenges [31,32]. In this regard, spatially referenced mobile phone data have emerged as a promising data source because of their extensive coverage, high penetration rate, and remarkable spatial–temporal continuity [33,34]. They adeptly capture the spatial distribution, mobility patterns, and social activities of the ambient population. Furthermore, mobile phone data have proven to be particularly efficacious in quantifying multifaceted attributes of the ambient population at finer spatiotemporal resolutions [32,35]. Although early research focused predominantly on estimating the number of ambient populations, recent methodological developments have broadened the scope of analysis to include multidimensional attributes of the ambient population, while ensuring the preservation of anonymity and desensitizing sensitive information to protect privacy [36]. In the domain of spatial equity evaluation, the identification of high-resolution proxies for socioeconomic status is paramount. To this end, a diverse array of data sources have been harnessed, including remote sensing [37], social media [38,39], and street view data [40]. The most recent research has leveraged machine learning methods to predict spatial variations in socioeconomic status at the neighborhood level, predicated

on online housing advertising text [41]. These endeavors demonstrate the feasibility of employing housing-related information as a metric for estimating the spatial distribution of socioeconomic status.

The primary objective of this study is to investigate the environmental inequality of PM_{2.5} pollution exposure among residents. Our goal is to delineate the spatial distribution patterns of PM_{2.5} concentrations and their association with the social strata and citizenship identities at a fine-scale level (1 km × 1 km). Xi'an, a representative industrial city in northern China, was selected as our study area. The technical route of this study is shown in Figure 1. Leveraging the kriging method, we generated the spatiotemporal distribution of PM_{2.5} concentration from daily air pollution monitoring data over a one-year period, from 1 January 2021 to 31 December 2021. Subsequently, we conducted an analysis of the spatiotemporal patterns of the environmental inequality of PM_{2.5} exposure, integrating data on the distribution of citizenship identities derived from mobile phone data with the distribution of social strata estimated through secondhand housing prices. The empirical findings highlight significant environmental inequality in PM_{2.5} exposure in Xi'an, with pronounced disparities observed among individuals of different social strata and citizenship identities.

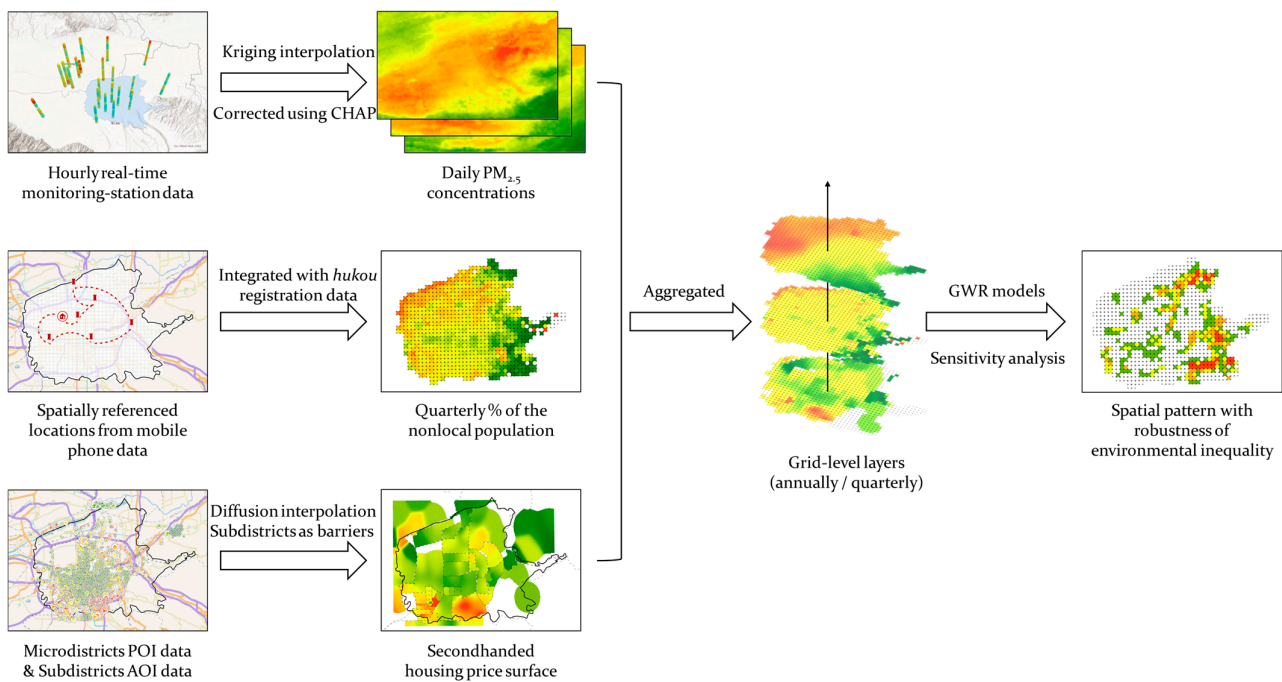


Figure 1. The flowchart of the study.

2. Materials and Methods

2.1. Study Area

The study area is the main urban area of Xi'an, situated within the Shaanxi Province of China. The region is located in the central Shaanxi Plain, nestled in the middle Yellow River Basin. As a quintessential industrial city, Xi'an boasts a diverse economic landscape, featuring key sectors such as infrastructure development, energy and chemical industries, and equipment manufacturing. Figure 2 shows the location of the study area in China.

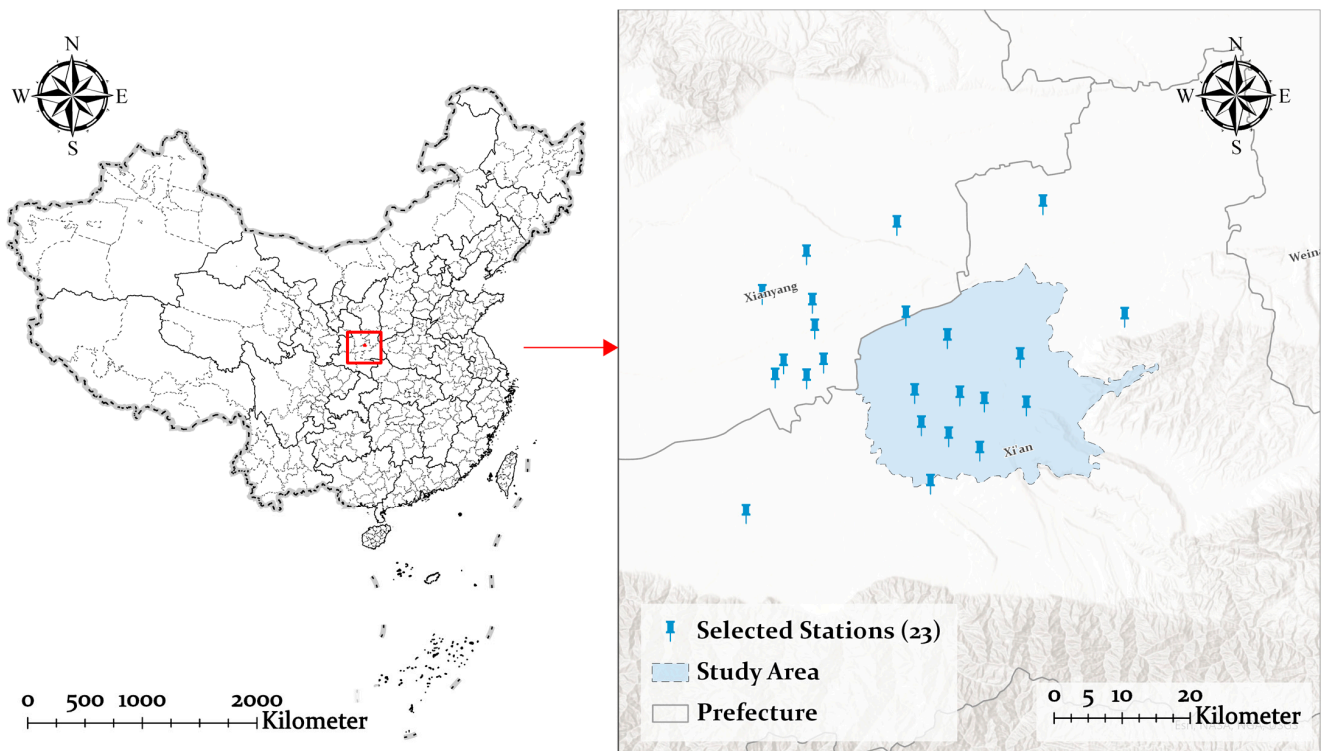


Figure 2. The location of the study area and selected air pollution monitoring stations.

2.2. Data

2.2.1. Air Pollution Data

In this investigation, we acknowledge the diurnal and seasonal fluctuations in human activities; accordingly, we employ a geostatistical method that leverages hourly real-time monitoring station data. To mitigate the constraints inherent in geostatistical analyses, we integrate a refined daily gapless $1 \text{ km} \times 1 \text{ km}$ global ground-level $\text{PM}_{2.5}$ dataset to enhance the accuracy of our estimates [42].

The air quality data were procured from the National Urban Air Quality Real-Time Release Platform of China (www.cnemc.cn) [43]. This dataset compiles hourly $\text{PM}_{2.5}$ concentrations, reading from an extensive network of 2024 monitoring stations in China. Considering proximity and topographical factors (as depicted in Figure 2), this study selected a subset of 23 monitoring stations situated within the study area and their immediate environs. Considering the significant perturbations in human behavior and atmospheric quality induced by the COVID-19 outbreak and consequent lockdown protocols in 2020 [44–46], our analysis is focused on the timeframe from 1 January 2021 to 31 December 2021.

The process of calculating the $\text{PM}_{2.5}$ dataset in this study is delineated as follows:

1. The hourly station data were aggregated, and the daily $\text{PM}_{2.5}$ concentrations during the entire day, daytime (9 a.m. to 6 p.m.), and nighttime (12 a.m. to 6 a.m.) were calculated for each station.
2. The kriging method was used to generate daily $\text{PM}_{2.5}$ concentrations throughout the entire day, daytime (9 a.m. to 6 p.m.), and nighttime (12 a.m. to 6 a.m.).
3. The estimated daytime and nighttime surfaces were corrected with the daily gapless $1 \text{ km} \times 1 \text{ km}$ global ground-level $\text{PM}_{2.5}$ dataset. For each cell:

$$CPM_{i,d,t} = UPM_{i,d,t} \times \frac{GHPM_{i,d}}{UPME_{i,d}} \quad (1)$$

where $CPM_{i,d,t}$ is the corrected $\text{PM}_{2.5}$ concentration for cell i during time t (daytime or nighttime) on day d , $UPM_{i,d,t}$ is the uncorrected $\text{PM}_{2.5}$ concentration for cell i during time t (daytime or nighttime) on day d , $GHPM_{i,d}$ is the daily $\text{PM}_{2.5}$ concentration for cell i on

day d according to the daily gapless 1 km global ground-level $PM_{2.5}$ dataset, and $UPME_{i,d}$ is the uncorrected entire day $PM_{2.5}$ concentration for cell i during day d .

2.2.2. Spatially Referenced Mobile Phone Data

In the sociopolitical fabric of China, the possession of a local *hukou* serves as a determinant of urban citizenship, fundamentally influencing an individual's eligibility for municipal public services [47]. Consequently, the *hukou* system is venerated as a pivotal metric for delineating citizenship identities. To attain precise measurements of *hukou* at a fine scale, this study employs spatially referenced mobile phone data, amalgamated with demographic and social activity data extracted from an anonymized cohort of users. This data consortium is procured through a collaborative endeavor with the Xi'an Public Security Bureau, which manages the data of all mobile phone users in Xi'an. Subjected to a stringent protocol of anonymization and aggregation, the data are distilled into a matrix of $1\text{ km} \times 1\text{ km}$ grid cells for analysis. The dataset encompasses key variables, including the percentage of nonlocal residents within the municipal confines of Xi'an, which is calculated as follows:

1. The historical locations during the daytime (i.e., 9 a.m. to 6 p.m.) were spatially mapped onto the grid cells, and the population within each grid was computed.
2. The historical locations during the nighttime (i.e., 12 a.m. to 6 a.m.) were spatially mapped onto the grid cells, and the population within each grid was computed.
3. The daytime population and nighttime population within each grid were combined and integrated with *hukou* registration data. The percentage of nonlocal residents within each grid is then determined as the percentage of residents with *hukou* registered in cities other than Xi'an relative to the total population within that grid.

Given the onerous computational demands of processing an entire annum of mobile phone data, a judicious balance was struck between computational complexity and analytical precision. To this end, we opted to focus on eight discrete and specific dates from the year 2021, selected to capture a spectrum of seasonal variations and weekly intervals. The chosen dates include 17 March (Wednesday), 20 March (Saturday), 16 June (Wednesday), 19 June (Saturday), 15 September (Wednesday), 18 September (Saturday), 24 November (Wednesday), and 27 November (Saturday). The selection of these dates is predicated on their representation of both weekdays and weekends, unencumbered by traditional Chinese festivals, which are known to induce aberrations in the typical spatial mobility patterns of individuals.

2.2.3. House Price Data

Relative residential property value, or housing price, is regarded as a socioeconomic status (SES) measure in geographical research [48]. Hence, this study uses the secondhand housing price per unit area as an indicator of neighborhood SES. The data were acquired from KE Holdings Inc., Beijing, China (also known as *Beike*), China's leading online and offline real estate brokerage and portal company, accessible via www.ke.com. Acknowledging the dynamic nature of real estate data subject to real-time market oscillations, this study meticulously selected housing price data that reflect the prevailing market conditions as of the 11th day of March in the year 2023, thereby ensuring the temporal relevance and accuracy of the SES indicators utilized in the analysis.

The house price data are stratified across two spatial hierarchical dimensions: (1) subdistricts, represented as polygon geometries; and (2) microdistricts, denoted as points. The term "subdistricts" refers to designated areas under the jurisdiction of local suburban governments. The term "microdistricts" alludes to enclosed areas with essential services provided within these gated communities and has been employed as a mechanism for smaller-scale administration by the Chinese government, as elucidated by Tomba [49]. These dual classifications provide critical stratigraphic signifiers for the spatially variable socioeconomic status and the segmentation of social collectives along the spectrum of social strata. Employing geostatistical interpolation techniques, this study harnesses subdistrict

boundaries as natural barriers and microdistricts as anchor points for the spatial modeling process. Consequently, the resultant house price surface is collapsed into a homogenized grid system, with each cell measuring 1 km × 1 km, thereby rendering the data amenable to subsequent analytical endeavors. This aggregation not only streamlines the dataset for tractable analysis but also preserves the nuanced spatial dynamics that are intrinsic to the socioeconomic landscape under investigation.

2.3. Dependent Variable and Independent Variables

In geographically weighted regression analysis (see Section 2.4.3), the dependent variable at the grid level is determined as follows:

- PM_{2.5} exposure is empirically quantified through the calculation of the mean PM_{2.5} concentration during both daytime and nighttime.

The independent variables include:

- Citizenship identity is measured by the percentage of the nonlocal population residing in a given grid.
- Social stratum is operationalized as socioeconomic status and measured by the mean price of secondhand houses within a particular grid.

2.4. Analytical Methods

2.4.1. Interpolation Techniques

The daily PM_{2.5} concentrations, in their unadjusted form, were estimated using the general kriging method. The kriging operations were executed within the ArcGIS Pro[®] 3.2 environment, with default parameter settings.

To establish the secondhand housing price surface, a diffusion interpolation with barriers was employed, wherein the boundaries of subdistricts function as barriers to the interpolation process. This computational procedure was also performed using ArcGIS Pro[®] 3.2.

2.4.2. Global and Local Spatial Autocorrelation

The Global Moran's I index is used as a diagnostic tool to assess the presence and strength of spatial autocorrelation. This metric quantifies the linear correlation between the values of a given variable within a specific geographic unit and the spatially weighted mean values of the same variable across neighboring geographic units. In our analysis, Global Moran's I was applied to quantify the degree of spatial autocorrelation observed in several important variables, including the percentage of nonlocal residents and housing prices. Furthermore, it was employed in the measurement of spatial autocorrelation within the residuals of the GWR (geographically weighted regression) model. To gain deeper insight into pinpointing clusters with high or low values, as well as identifying spatial outliers, we further employed Anselin Local Moran's I, also known as cluster and outlier analysis. The global Moran's I and Anselin Local Moran's I were calculated using ArcGIS Pro[®] 3.2.

2.4.3. Geographically Weighted Regression

The primary aim of this paper is to uncover spatial inequities in PM_{2.5} exposure, with a particular focus on identifying areas where there exists a positive correlation between the percentage of the nonlocal residents (a proxy for citizenship identity) and PM_{2.5} concentration levels, and, conversely, areas where there is a negative correlation between the average housing price (a proxy for social stratum) and PM_{2.5} concentration. To achieve this, it is imperative to employ an algorithm capable of detecting localized patterns among these variables.

Geographically weighted regression (GWR) facilitates the exploration of varying relationships between independent and dependent variables across locales [50,51]. In this study, we employed GWR to elucidate the spatially varying relationships between PM_{2.5}

exposure and two key independent variables: the percentage of the nonlocal population and the average housing price. The GWR model computes localized estimates of β_p at each location i by utilizing the centroids associated with the grid data. The construction of three models are as follows.

Model 1: The mathematical representation of the model regarding daytime PM_{2.5} concentrations and the nonlocal population is as follows:

$$y_i = \beta_{i0} + \beta_{i1}X_{i1} + \varepsilon_i \quad (2)$$

where y_i denotes the daytime PM_{2.5} concentration at grid i in 2021, X_{i1} denotes the percentage of the nonlocal population at grid i in 2021, β_{i0} denotes the localized realization of the constant at grid i , β_{i1} denotes the localized realization of the coefficient of the percentage of the nonlocal population at grid i , and ε_i denotes the localized realization of the error item at grid i .

Model 2: The mathematical representation of the model regarding nighttime PM_{2.5} concentrations and the nonlocal population is the same as Equation (2), but y_i denotes the nighttime PM_{2.5} concentrations at grid i in 2021.

Model 3: The mathematical representation of the model for nighttime PM_{2.5} concentrations and the housing price follows Equation (2), where y_i denotes the nighttime PM_{2.5} concentration at grid i in 2021, and X_{i1} denotes the average housing price at grid i in 2021.

Given that the urban population typically gravitates towards the city center for employment and leisure activities during daytime hours, giving rise to an inconsistency between the population and their residences, the model regarding daytime PM_{2.5} concentrations and the housing price is not applicable and will not be fitted.

To estimate the models, we leveraged the package “spgwr” in the R programming environment (version 4.1.3), as detailed by Bivand [52]. The “gwr.sel” function from the “spgwr” package is invoked to ascertain the optimal bandwidth selection for the GWR models.

2.4.4. Sensitivity Analysis

Given that the estimation of the nonlocal residents at each grid for the year 2021 is predicated on a mere eight-day sample, it is important to apply a sensitivity analysis to determine whether the choice of which days to select has an impact on the results. Hence, we fit the following quarter-specific models:

Model 4: The mathematical representation of the quarter-specific relationship between daytime PM_{2.5} concentrations and the nonlocal population is as follows:

$$y_{i,q} = \beta_{i0,q} + \beta_{i1,q}X_{i1,q} + \varepsilon_{i,q} \quad (3)$$

where $y_{i,q}$ denotes the daytime PM_{2.5} concentration at grid i in quarter q , $X_{i1,q}$ denotes the percentage of the nonlocal population at grid i in quarter q , $\beta_{i0,q}$ denotes the localized realization of the constant at grid i in quarter q , $\beta_{i1,q}$ denotes the localized realization of the coefficient of the percentage of the nonlocal population at grid i in quarter q , and $\varepsilon_{i,q}$ denotes the localized realization of the error item at grid i in quarter q .

Model 5: The mathematical representation of the quarter-specific relationship between nighttime PM_{2.5} concentrations and the nonlocal population is formed in the same way as Equation (3), but where $y_{i,q}$ denotes the nighttime PM_{2.5} concentrations at grid i in quarter q ; the others remain the same as in Model 4.

Finally, we construct a pattern robustness indicator to describe the robustness of the detected inequality pattern regarding the citizenship identities in each grid, given as

$$R_{t,i} = \sum_{q=1}^4 Sig_{t,q,i} \quad (4)$$

where $R_{t,i}$ refers to the pattern robustness of grid i for timespan t (daytime or nighttime), and $Sig_{t,q,i}$ is defined as

$$Sig_{t,q,i} = \begin{cases} 1, & b_{t,q,i} > 0 \text{ and is significant} \\ 0, & \text{otherwise} \end{cases} \quad (5)$$

where $b_{t,q,i}$ refers to the localized realization of the coefficient of the percentage of the nonlocal population at grid i in quarter q for timespan t (i.e., daytime or nighttime, coming from Model 4 and Model 5, respectively). The level of significance was set to 0.05.

The sensitivity analysis was also performed in the R programming environment (version 4.1.3), with the “spgwr” package.

3. Results

3.1. The Spatiotemporal Patterns of the PM_{2.5} Concentration

As illustrated in Figure A1, by 2021, the prevailing conditions in Xi’an had largely returned to prepandemic norms. Hence, it is reasonable to examine the PM_{2.5} concentration in 2021 in this study.

Figure 3 presents the daily estimated PM_{2.5} concentration in Xi’an throughout 2021, subdivided into three panels representing the entire day, daytime, and nighttime. Notably, Friday exhibits the peak PM_{2.5} concentration levels, whereas Monday exhibits the lowest concentration (excluding during the daytime) over the course of the week. Figure 3 further signifies a progressive increase in concentrations from Monday to Friday, followed by a subsequent decrease from Friday to the ensuing Monday.

In terms of seasonal fluctuations, PM_{2.5} concentrations typically increase from late fall through early spring, encompassing a five-month period from November to March. During this interval, the recorded concentrations predominantly align with the Interim Target 2, with values ranging from 37.5 to 50 µg/m³ and even more severe concentrations. These values are juxtaposed against the “recommended long- and short-term AQG levels and interim targets” as stipulated by the World Health Organization [53]. Conversely, from mid-May to mid-October, concentrations tend to be relatively lower, primarily falling within the range of the AQG level (0 to 15 µg/m³) and Interim Target 3 (25 to 37.5 µg/m³). Figure A2 presents the corresponding results according to the ambient air quality standards issued by the Ministry of Ecology and Environment of the People’s Republic of China [54].

Figure 4 shows the spatial distribution of the PM_{2.5} concentration in Xi’an for the year 2021. It visualizes both annual data and quarterly variations. With respect to the annual tendencies, heightened PM_{2.5} concentrations are noted in the northwestern sectors of the city, whereas comparatively diminished levels are observed in the southeastern reaches. During the nighttime, PM_{2.5} concentrations are higher in the northwest and lower in the southeast of the city, while PM_{2.5} concentrations are higher in the center of the city in the daytime. In the southeast, the daytime and nighttime concentrations are relatively similar. Conversely, the daytime concentrations are significantly lower than the nighttime concentrations in the northwest.

Quarterly fluctuations in the spatial distribution patterns of the PM_{2.5} concentration are observed. In the first quarter, the distribution pattern shows higher concentrations in the west and lower concentrations in the east. In the second and third quarters, a southward dip in concentrations is observed, with concentrations radiating outward to the surrounding areas. In the fourth quarter, the distribution pattern aligns with the annual trend, exhibiting lower concentrations in the southeast and higher concentrations in the northwest. According to the analysis of diurnal variations, significant differences existed between daytime and nighttime concentrations in the first and fourth quarters. In the second and third quarters, the daytime and nighttime concentrations exhibit less pronounced differences; however, the nighttime concentrations in the southern part of the city are surprisingly lower than the daytime concentrations, which is contrary to the observed annual pattern. Furthermore, the daytime PM_{2.5} concentrations are greater than

the nighttime PM_{2.5} concentrations in the third quarter, which is also contrary to the observed annual pattern.

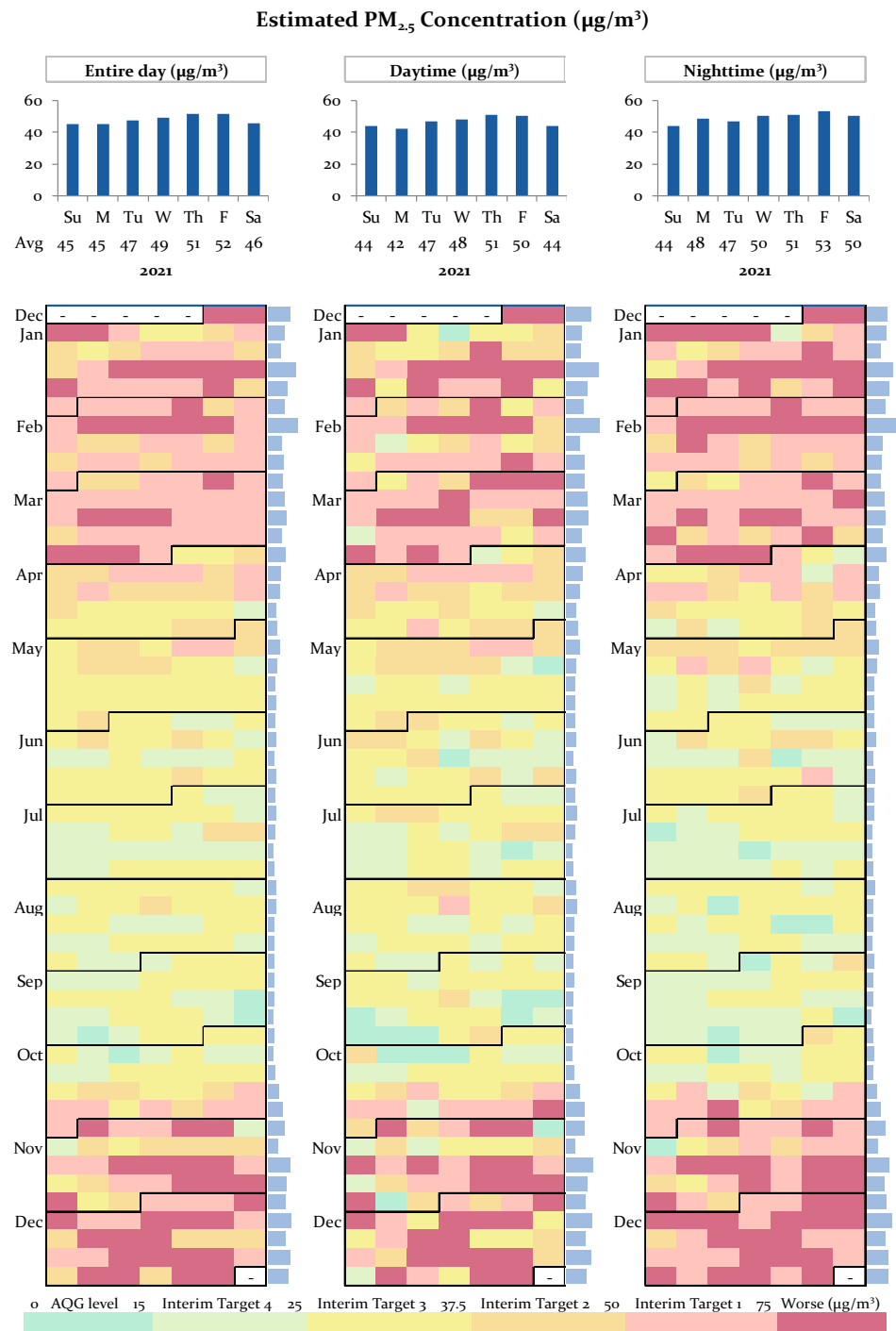


Figure 3. Temporal distribution of the PM_{2.5} concentration across 2021, depicting the daily, weekly, and weekly mean variations in the PM_{2.5} concentration. The breaks and labels of PM_{2.5} concentration adhere to the guidelines established by the World Health Organization [53]. The “entire day” corresponds to 00:00 to 23:59; “daytime” spans from 9 a.m. to 6 p.m.; and “nighttime” encompasses the hours from 12 a.m. to 6 a.m. The definitions of daytime and nighttime align with those used for mobile phone data. This chart was created using the Calendar Chart Template from Vertex42.com [55].

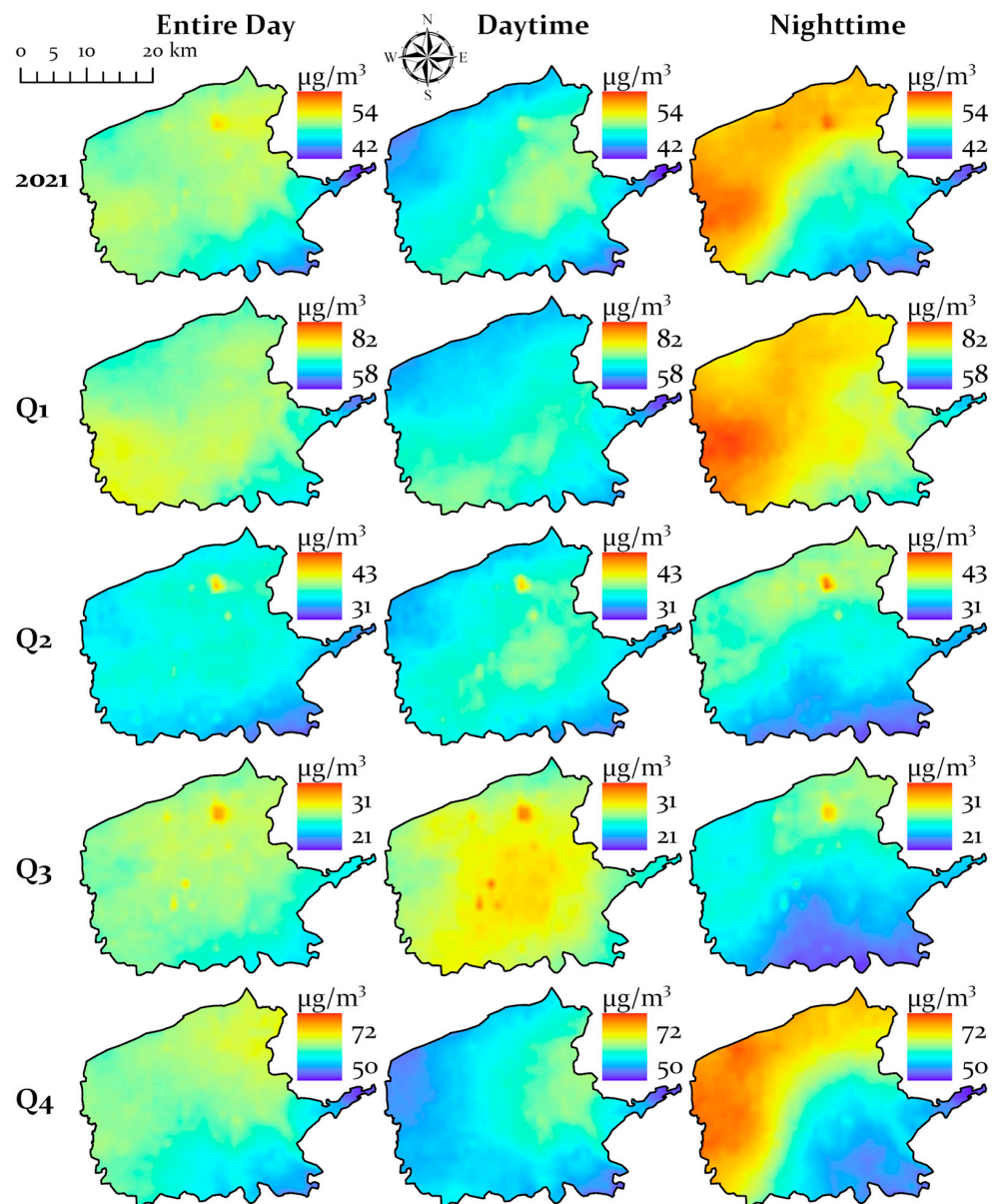


Figure 4. Spatial distribution of the PM_{2.5} concentration in Xi'an in 2021. To account for the significant differences among quarters, the color bar ranges are consistent within each quarter (or for annual subplots). Q1 to Q4 refer to quarters 1 to 4, respectively. The “entire day” corresponds to 00:00 to 23:59; “daytime” spans from 9 a.m. to 6 p.m.; and “nighttime” encompasses the hours from 12 a.m. to 6 a.m. The definitions of daytime and nighttime align with those used for mobile phone data.

3.2. Environmental Inequality in Terms of PM_{2.5} Exposure

Figure 5 illustrates the spatial distribution of the percentage of nonlocal residents in the four quarters of 2021 and housing price (CNY/m²) for the same year. The spatial distribution of the percentage of nonlocal residents reveals a distinct pattern, with elevated values in the northwestern sector and diminished values in the southeastern sector. Housing prices display a characteristic centralized distribution pattern. Notably, three clusters with low values are observed in the northwestern, northern, and eastern sections of the urban area, while the southern and northeastern parts of the city exhibit three clusters with high-value concentrations.

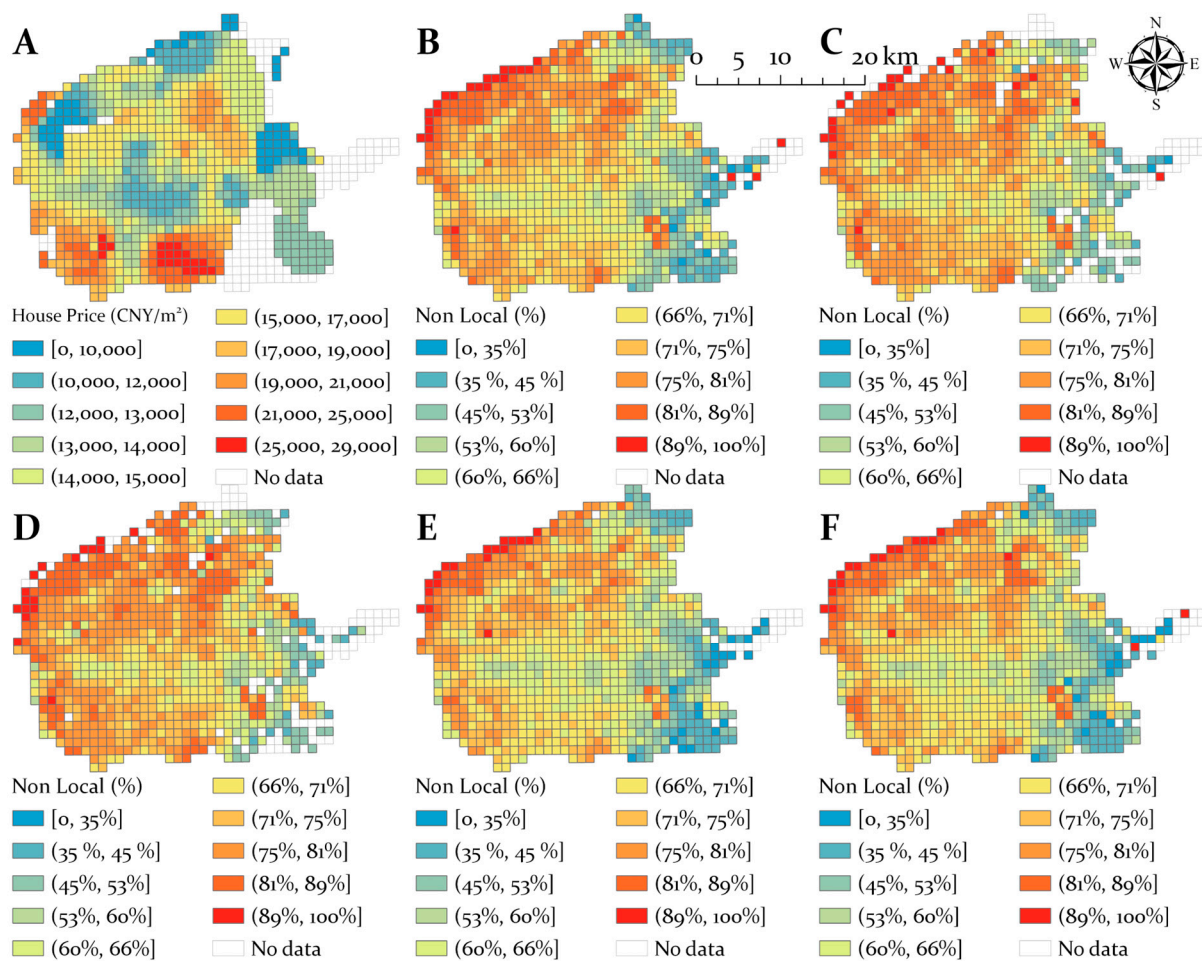


Figure 5. Spatial distributions of the independent variables. (A) The estimated housing price in 2021 (using data from 11 March 2023); (B) the percentage of nonlocal residents in 2021; (C) the percentage of nonlocal residents in 2021 quarter 1; (D) the percentage of nonlocal residents in 2021 quarter 2; (E) the percentage of nonlocal residents in 2021 quarter 3; (F) the percentage of nonlocal residents in 2021 quarter 4.

As indicated in Table 1 and Figure 6, the percentage of nonlocal residents and the housing price both exhibit significant global and local spatial autocorrelation, suggesting the reasonableness of using GWR models. Figure A3 displays the bivariate relationship between independent and dependent variables, suggesting the potential for both linear and polynomial relationships. In response to this, an exhaustive enumeration of parameter combinations was conducted, encompassing variable relationships (linear, quadratic, or cubic) and bandwidth parameters (including bandwidth adaptivity, optimization method, and geographical weighting function). A comparative assessment of their goodness of fit was executed, with the findings presented in Table S1. The results reveal that the incorporation of polynomial relationships does not confer a superior fit for the models. Consequently, linear models, specifically Models 1, 2, and 3, as per Equation (2), were selected for their optimal balance of fit and interpretability. The parameters of these chosen models are presented in Table S2.

Table 1. Global Moran's I of independent variables.

Variable	Moran's I	Z Score	p Value
Estimated housing price in 2021	0.751	62.665	0.000
Percentage of nonlocal residents in year 2021	0.652	58.688	0.000
Percentage of nonlocal residents in 2021 quarter 1	0.600	50.443	0.000
Percentage of nonlocal residents in 2021 quarter 2	0.628	52.484	0.000
Percentage of nonlocal residents in 2021 quarter 3	0.730	65.472	0.000
Percentage of nonlocal residents in 2021 quarter 4	0.650	58.252	0.000

Parameters used in ArcGIS Pro tool Spatial Autocorrelation (Global Moran's I) (Spatial Statistics Tools): Conceptualization of Spatial Relationships: FIXED_DISTANCE_BAND; Distance Method: EUCLIDEAN_DISTANCE; Standardization: ROW; Distance Band or Threshold Distance: 2341.

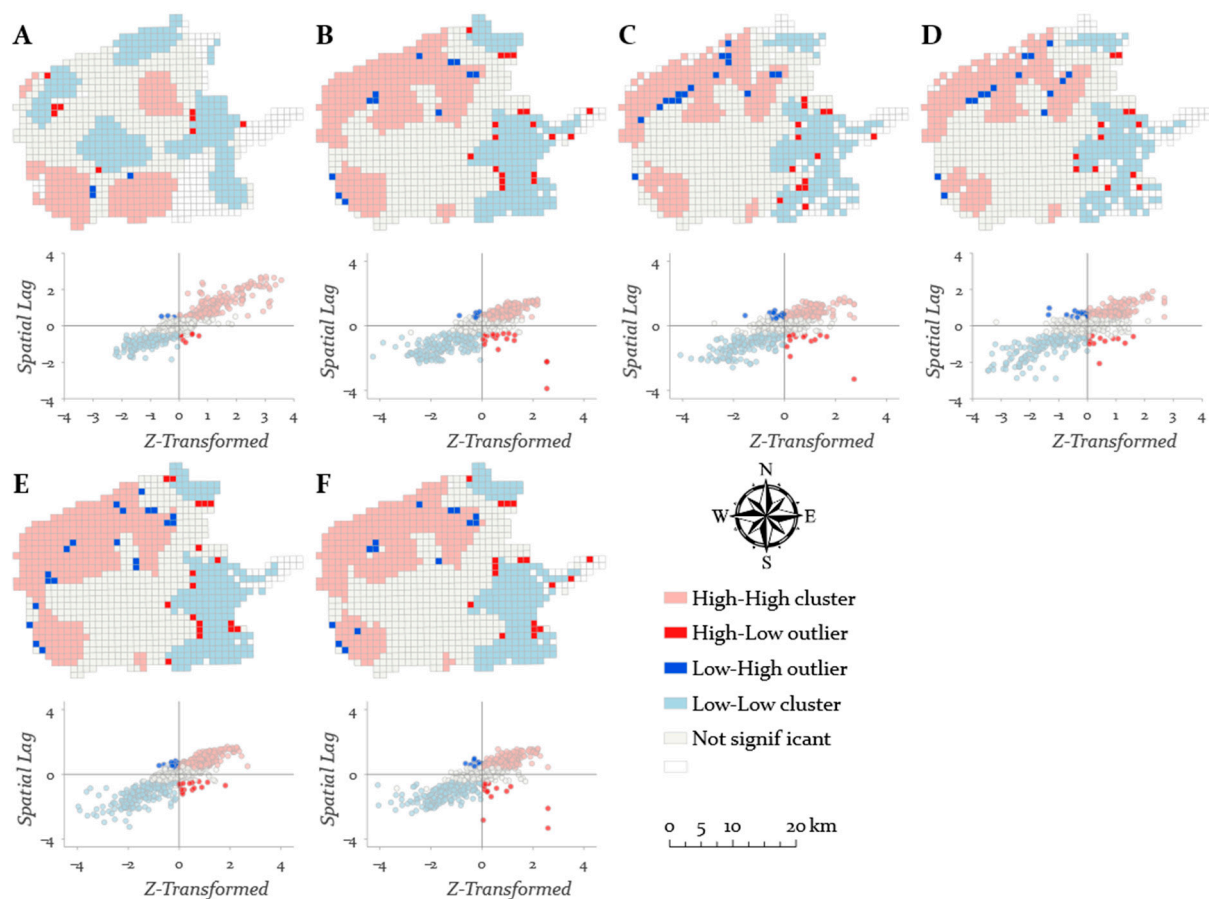


Figure 6. Moran's scatterplots and Anselin Local Moran's I for the independent variables. (A) The estimated housing price in 2021 (using data from 11 March 2023); (B) the percentage of nonlocal residents in 2021; (C) the percentage of nonlocal residents in 2021 quarter 1; (D) the percentage of nonlocal residents in 2021 quarter 2; (E) the percentage of nonlocal residents in 2021 quarter 3; (F) the percentage of nonlocal residents in 2021 quarter 4.

Figure 7A–C present the results of GWR models investigating spatiotemporal patterns of inequality in $PM_{2.5}$ exposure, regarding the percentage of nonlocal residents and housing prices, across the city. Positive significance indicates greater $PM_{2.5}$ exposure in areas with a greater percentage of nonlocal residents, as shown in Figure 7A,B. Conversely, negative significance denotes areas with reduced housing prices correlating with increased $PM_{2.5}$

exposure, as shown in Figure 7C. The inequality related to the percentage of nonlocal residents is particularly pronounced in the northwestern and southern sectors of the city, which are characterized by lower housing prices, as identified in Figure 5. The inequality related to housing prices is observed in various urban regions, indicating a more complex spatial dynamic. Figure 7D,E graphically represent the robustness of the inequality pattern (i.e., significant outcomes observed in quarterly regressions), particularly focusing on the daytime and nighttime percentages of nonlocal residents exposed to $PM_{2.5}$, respectively. The consistency of spatial distributions of daytime and nighttime $PM_{2.5}$ exposure inequality patterns across different quarters suggests the robustness of the observed trends. Notably, nighttime patterns display more enhanced robustness than daytime patterns. Hence, Figure 7D,E illustrate that the choice of which days to select has a slight impact on the results presented in Figure 7A,B.

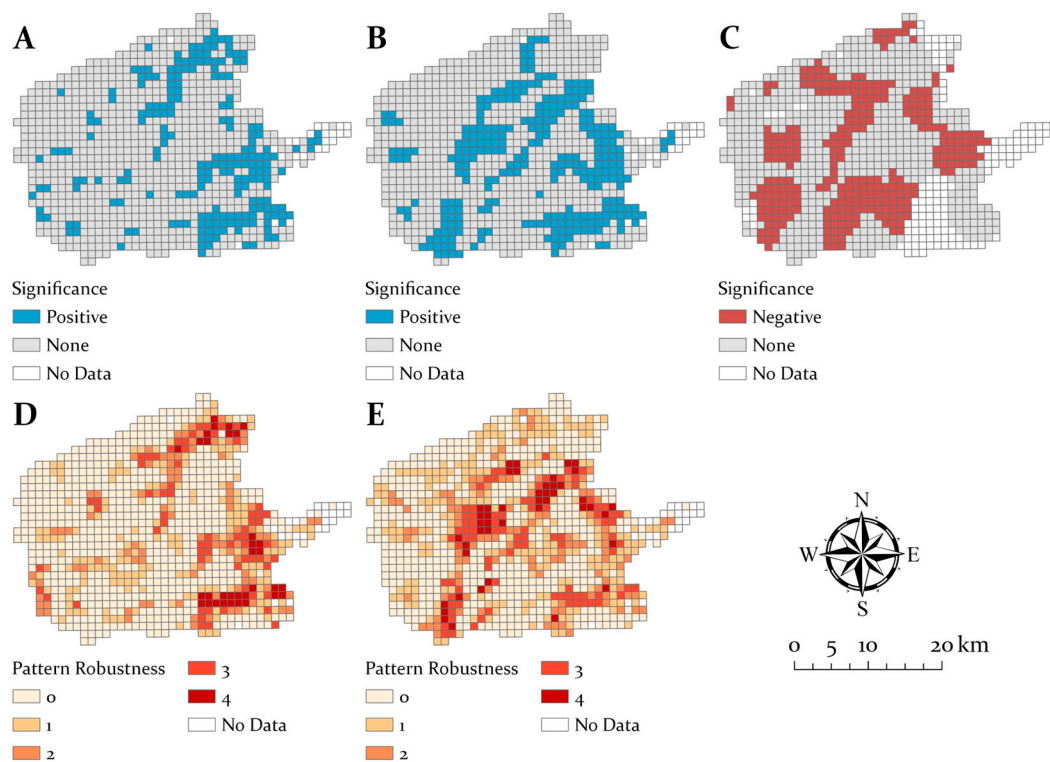


Figure 7. Localized $PM_{2.5}$ exposure inequality pattern and sensitivity analysis. (A) Results of Model 1, regarding daytime $PM_{2.5}$ concentration and the percentage of nonlocal population. (B) Results of Model 2, regarding nighttime $PM_{2.5}$ concentration and the percentage of nonlocal population. (C) Results of Model 3, regarding nighttime $PM_{2.5}$ concentration and the secondhand housing price. (D) Sensitivity analysis based on Model 4, regarding daytime $PM_{2.5}$ concentration and the percentage of nonlocal population in quarterly data. (E) Sensitivity analysis based on Model 5, regarding nighttime $PM_{2.5}$ concentration and the percentage of nonlocal population in quarterly data.

4. Discussion

4.1. Principal Findings

This study conducted a microscale analysis of $PM_{2.5}$ exposure variability within Xi'an city, leveraging housing price and mobile phone data to explore the correlation between $PM_{2.5}$ concentrations and pivotal social determinants: citizenship identity and socioeconomic status. The findings indicate that residents lacking local registration exhibit increased exposure to $PM_{2.5}$. Additionally, the research uncovers a mitigating effect of elevated socioeconomic status, which may afford individuals the agency to select residences in areas with reduced $PM_{2.5}$ concentrations. This suggests a social gradient in air pollution exposure, with implications for environmental justice and urban planning.

4.2. Comparison with Previous Work

This research augments the burgeoning literature on environmental inequality in the context of air pollution exposure. A number of recent studies have endeavored to elucidate the environmental inequality in air pollution exposure in China [10,22–25,30]. At the macroscale (e.g., national scale), existing studies have predominantly discovered correlations between spatial distribution of PM_{2.5} concentration and regional population density and land cover types, among several others [28,56].

At the urban scale, research (e.g., studies focused on Beijing, Nanjing and Wuhan) has found the association between PM_{2.5} concentration and walkability of streets, land uses, and found that air pollution exposure risks for children and the elderly are uneven [10,23,57]. Studies in China found that the risk of PM_{2.5} exposure varies with age, income, gender, etc. [22,57]. Notably, the elderly, who experience higher risk of air pollution exposure, are mainly located in the central and peripheral urban zones [10]. J. Chen et al. [58] found that risk of environmental pollution exposure of residents varies with migration status, and migrants from rural places have higher risk of environmental pollution exposure. However, the study was aimed at the national scale, and there is a lack of understanding of the microscale variation within the city.

Our study bridges this gap by dissecting the environmental inequality in PM_{2.5} exposure at grid scale. We have unveiled the spatial distribution of PM_{2.5} concentration and their associations with social strata and citizenship identity of the ambient population at a grid scale. This microscale analysis complements the national-level studies by extending the discourse to include the intricate relationship between an individual's socioeconomic status and citizenship, and their exposure to air pollution risks. This approach provides a more nuanced understanding of environmental inequality, transitioning from a macroscopic perspective to a more localized scale.

4.3. Practical Implications

Our findings suggest that the observed environmental inequality in PM_{2.5} exposure in Xi'an can be partly attributed to historical and ongoing disparities in urban planning. While the specific reasons behind these disparities require further investigation, our analysis of the city's general master plan (2008–2035) reveals a persistent neglect of the northwestern sector, characterized by an absence of environmental amenities, such as green belts, and a dearth of access to vital public services [59,60]. This neglect has rendered the area's residents susceptible to the adverse effects of air pollution, reflecting a broader pattern of environmental injustice where marginalized communities are disproportionately affected by environmental hazards.

The spatial distribution of PM_{2.5} exposure may also be influenced by social dynamics, with nonlocal residents potentially forming residential clusters due to weaker social ties or cultural integration with the local community [61,62]. The concentration of nonlocal residents in the northwestern district, exacerbated by limited policy focus and economic development, further contributes to the environmental inequality.

To address these intertwined issues, a comprehensive and multifaceted strategy is warranted:

Housing affordability issue in less polluted areas. Introduce financial assistance programs and subsidies aimed at making housing in less polluted areas accessible to low-income nonlocal residents. Additionally, invest in affordable housing development in less polluted areas to alleviate the concentration of vulnerable populations near pollution sources.

Mitigating pollution sources in the northwestern district. Implement stricter environmental regulations for industries in the northwestern district to curtail PM_{2.5} emissions. Promote sustainable development through investment in clean technologies and alternative energy sources, and consider the strategic relocation of polluting industries to less populated industrial zones.

Enhancing public services in less developed areas. Direct investment towards infrastructure improvements in underdeveloped areas, with an emphasis on public transportation, healthcare facilities, and educational opportunities. The development of green spaces and parks can simultaneously enhance air quality and offer residents access to recreational spaces.

Promoting social integration and reducing discrimination. Enact antidiscrimination policies to protect nonlocal residents from biased housing practices, and ensuring equitable access to opportunities regardless of their citizenship status. Encourage social integration programs to build a cohesive community with a collective commitment to environmental health.

Utilizing environmental justice frameworks in urban planning. Embed principles of environmental justice into urban planning frameworks to ensure a just distribution of environmental resources and to mitigate the disparate impacts of environmental hazards across different socioeconomic and citizenship groups. Mandate comprehensive environmental impact assessments for new developments to evaluate and balance air quality implications and environmental benefits equitably.

These policy recommendations, grounded in the study's findings, necessitate a nuanced understanding of local contexts, collaborative efforts among diverse stakeholders, and vigilant monitoring to ensure their efficacy in redressing environmental inequalities.

4.4. Strengths and Limitations

This study presents a useful attempt to quantitatively evaluate the fine-scale disparities in air pollution exposure predicated on social strata and citizenship identity. Our empirical study affirms the viability of examining the spatial variation of air pollution exposure at grid scale. Two important measures, citizenship identity and social stratum, can be quantified using mobile phone big data. To be specific, the citizenship identity can be quantified using the percentage of nonlocal population residing in a grid, and social stratum can be operationalized as socioeconomic status and measured by the average price of secondhand houses within in a grid.

Despite the study's contributions, it is circumscribed by limitations that set the stage for future research. The findings are limited to the grid scale, which warrants exploration of more discrete geographical entities such as subdistricts and microdistricts to attain a heightened level of granularity. Additionally, the research's scope did not encompass occupational-based inequalities due to an absence of professional data on residents, underscoring the need for multifaceted data sources in subsequent studies.

The utilization of housing prices as an index of socioeconomic status is not without its challenges, particularly given the constraints in procuring data for the year 2021. The COVID-19 pandemic's variegated effects on housing prices further complicate the use of 2023 data as a proxy for the preceding year. While the robust correlation coefficient of 0.7449 between the average housing prices of 2021 and March 2023 at the subdistrict level substantiates the study's data strategy (as detailed in Appendix B), the acquisition of historical data remains an imperative for future research endeavors.

Furthermore, the calculation of the nonlocal resident ratio is currently anchored in data from a mere eight days, casting uncertainty over the established weekday-weekend pattern. Although sensitivity analysis indicates minimal impact from the specific days selected, a more expansive temporal framework is advisable for future research to solidify this metric. Lastly, the potential influence of unaccounted confounding factors on PM_{2.5} exposure cannot be discounted, necessitating the integration of a wider array of variables in forthcoming studies to deepen our comprehension of this intricate phenomenon.

5. Conclusions

This study elucidates the environmental inequality pertaining to PM_{2.5} exposure in Xi'an, with a particular focus on the inordinate burden shouldered by nonlocal residents in the city's northwestern quadrant. A stark contrast is observed in the PM_{2.5} concentrations

experienced by these residents as opposed to those inhabiting the southern regions, who are generally characterized by higher socioeconomic status and are favored with improved air quality. Our paper identifies citizenship identity and social strata as key factors contributing to the observed inequality. Furthermore, we explored potential underlying causes related to historical and ongoing disparities in urban planning and the *hukou* system, which can limit access to opportunities and resources based on residency status. This research contributes to a growing body of knowledge on environmental justice, highlighting the complex interplay between social and spatial factors in shaping environmental exposure risks.

In sum, this research provides a spatial lens through which to view the social inequalities engendered by identity, power, and economic factors, as reflected in PM_{2.5} exposure levels in Xi'an. By acknowledging the limitations and identifying areas for future research, this study sets the stage for the advancement of efficacious strategies aimed at redressing environmental inequalities and promoting a more just and equitable urban milieu that is sensitive to the environmental rights and wellbeing of all its inhabitants.

Supplementary Materials: The following supporting information can be downloaded at: <https://www.mdpi.com/article/10.3390/ijgi13070257/s1>, Figure S1: Bivariate relationship between PM_{2.5} concentration and the percentage of nonlocal population; Table S1: Parameter and goodness of fit of all models; Table S2: Parameter and goodness of fit of selected models.

Author Contributions: Conceptualization, Li He; methodology, Li He and Lingfeng He; software, Lingfeng He; validation, Li He and Lingfeng He; formal analysis, Li He and Lingfeng He; investigation, Li He, Lingfeng He, Zhongmin Wang, Ping An, and Min Liu; resources, Li He and Lingfeng He; data curation, Lingfeng He, Zhongmin Wang, Ping An, and Min Liu; writing—original draft preparation, Li He, Lingfeng He, Zezheng Lin, Yao Lu, and Shurui Gao; writing—review and editing, Li He, Lingfeng He, Zezheng Lin, Chen Chen, and Jie Xu; visualization, Li He and Lingfeng He; supervision, Li He; project administration, Li He; funding acquisition, Li He. Li He and Lingfeng He contributed equally to this work. All authors have read and agreed to the published version of the manuscript.

Funding: This research was funded by the Ministry of Education, Humanities and Social Sciences Research Youth Foundation, China (No. 20YJC840014), the National Natural Science Foundation of China (No. 42001164), and Research Project on Forging a Sense of Community for the Chinese Nation in Shaanxi Province (No. 2024MZW001). The APC was funded by the Ministry of Education, Humanities and Social Sciences Research Youth Foundation, China (No. 20YJC840014) and the National Natural Science Foundation of China (No. 42001164).

Data Availability Statement: Mobile phones are not available due to the information security requirements. House price data and code used in data collection, data processing, and data analysis are available via <https://github.com/CenterForSocialComputing/ijgi-spatial-inequality-of-PM2.5-exposure>.

Conflicts of Interest: The authors declare no conflicts of interest.

Appendix A. Explanation of Variables Selection

For residents in China's big cities, whether they hold a household registration system is an important factor in whether they can buy a home and in which geographical area they can buy a home. The *hukou* system pointed out in this paper as a phenomenon of social strata division in China's big cities has been proved by many existing studies (e.g., [63–65]). The impact on the purchase of housing is mainly reflected in the following aspects:

Whether residents have local *hukou* directly affects the eligibility of residents to buy a house. Since the 2010s, all major cities have had limited home purchase policies. Most big cities have restrictions on who can buy a home, and one of the most important restrictions is household registration. Nonresidents usually need to meet certain conditions to buy a home, such as paying local social security or personal income taxes for a certain number of years. The vast majority of mainstream cities only allow qualified nonresident residents to settle down and, thus, qualify for a house purchase.

In addition, even for some urban residential areas which can allow nonregistered people to buy homes, they still bear higher loan rates and down payments than registered residents. For example, *Notice of the People's Bank of China on Adjusting the Policy on Personal Housing Loans* [66] stipulates that the down payment ratio of nonregistered residents to buy a first home shall not be less than 35%, and the loan interest rate shall not be less than 1.1 times the benchmark interest rate. Another example is *Notice on Adjusting and Optimizing the Standards for Ordinary Housing and Personal Housing Loan Policies in Beijing* [67], which stipulates that nonhousehold resident families must pay social security or personal income tax for five consecutive years when purchasing a house in Beijing.

Another example is that in the same city, different residents enjoy completely different public services. Registered residents can enjoy more public services, such as children's education and medical security. For example, *the Compulsory Education Law of the People's Republic of China* stipulates that school-age children and adolescents at the stage of compulsory education shall only receive education in schools where their "hukou registration is located". In addition, in many mainstream cities, many benefits, including pension insurance and unemployment insurance, are also highly tied to household registration.

Finally, the segregation of economic and social status caused by the household registration system causes the different economic status of different groups, and also affects the economic ability of more nonlocal residents to buy property in areas with better public services. The first is the barrier to migration: the household registration system restricts the freedom of migrant workers. Many are unable to move to higher-paying areas and attain better-paying formal jobs. Forced to perform more manual labor in big cities, they are confined to the primary labor market, known as "migrant workers", and are destined to struggle to buy better-served property. The existing high housing prices may cause the labor force to be unable to find long-term stable employment in the place of employment, and further aggravate the differentiation of social strata.

Appendix B. Explanation of Using House Price Data in 2023

Currently there are two methods to obtain the house price data: (1) online map services (e.g., API of Ke.com), and (2) the list of house sales (e.g., Web Pages of Anjuke.com). The advantage of Method 1 is that the collected data contain spatially referenced information that can be spatially matched with other spatial data used in this analysis, whereas the disadvantage is that we can only obtain real-time house prices; the historical house price data are not available. Method 2, on the contrary, is characterized by its capacity to yield historical data. However, this method is encumbered by the limitation that the data procured lack spatial referencing, a critical component for spatial analysis. Moreover, despite the inclusion of geographic textual descriptors within the dataset obtained through Method 2, the nonstandardized structure of this textual information poses significant challenges. The alignment of such data with that derived from Method 1 is rendered infeasible owing to these structural discrepancies. Additionally, the prevalent challenges associated with geocoding in the context of Chinese-based geospatial data are widely acknowledged within both industrial and academic spheres. Consequently, after a thorough evaluation of the methodological constraints and data integrity considerations, the utilization of data sourced via Method 2 was deliberately eschewed in favor of alternative datasets that better align with the spatial analysis requirements of our research.

As supplementary support for adopting Method 1, we conducted a correlation analysis on the historical data obtained through Method 2. These are subdistrict-level data, and after removing missing values, a total of $N = 118$ subdistricts located in the study area were taken into analysis. In the correlation analysis, X is the housing price of the subdistrict in March 2023, and Y is the average housing price of the subdistrict in 2021. We find that the correlation between X and Y is 0.7449. The high degree of linear correlation ensures the validity of the direction and significance of the GWR coefficients, as we only focus on the relative size of the coefficients rather than absolute size. This can serve as proof of the rationality of our data collection method.

Appendix C. Figures

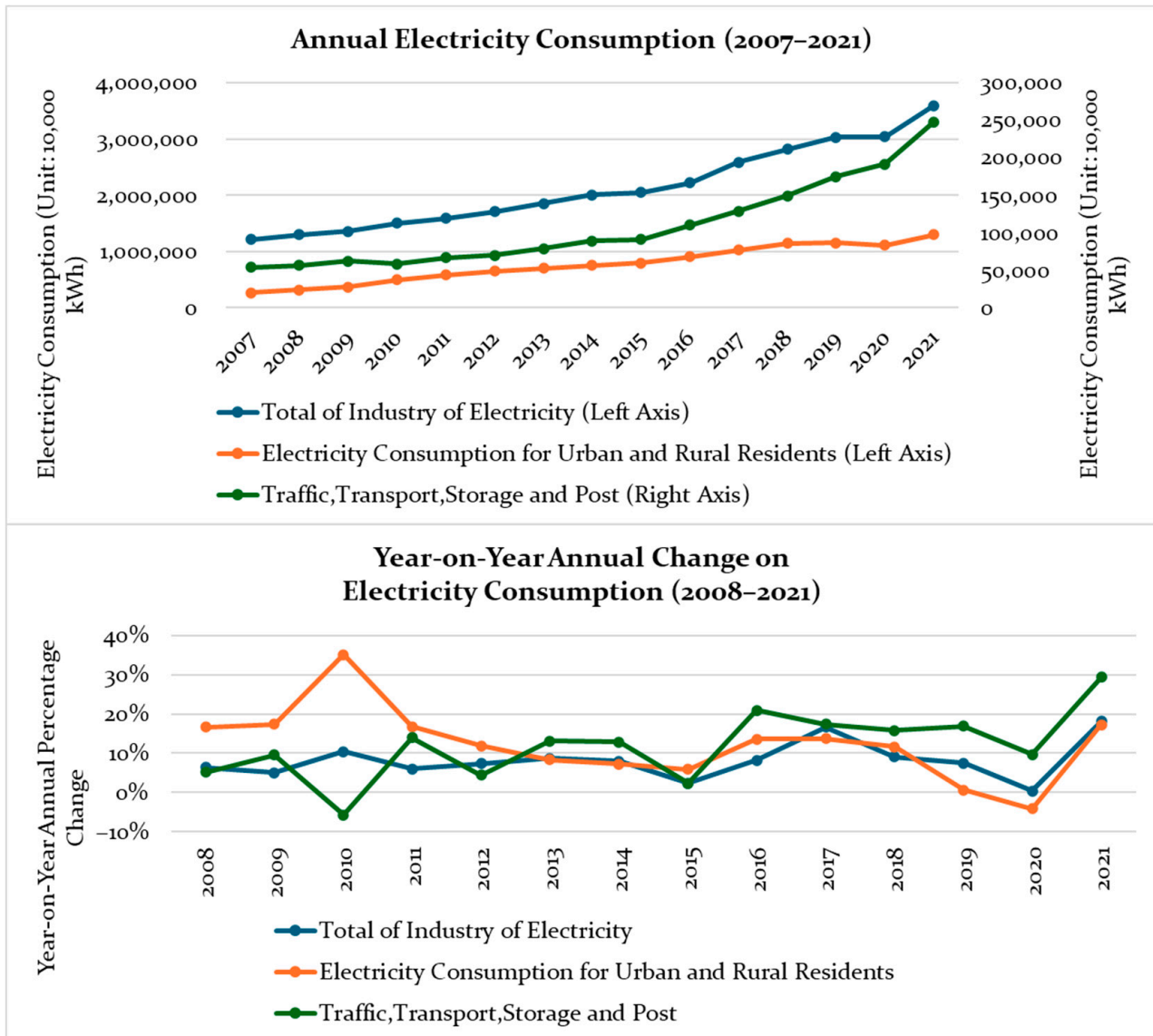


Figure A1. The annual electricity consumption and its year-on-year annual change from 2007 to 2021.

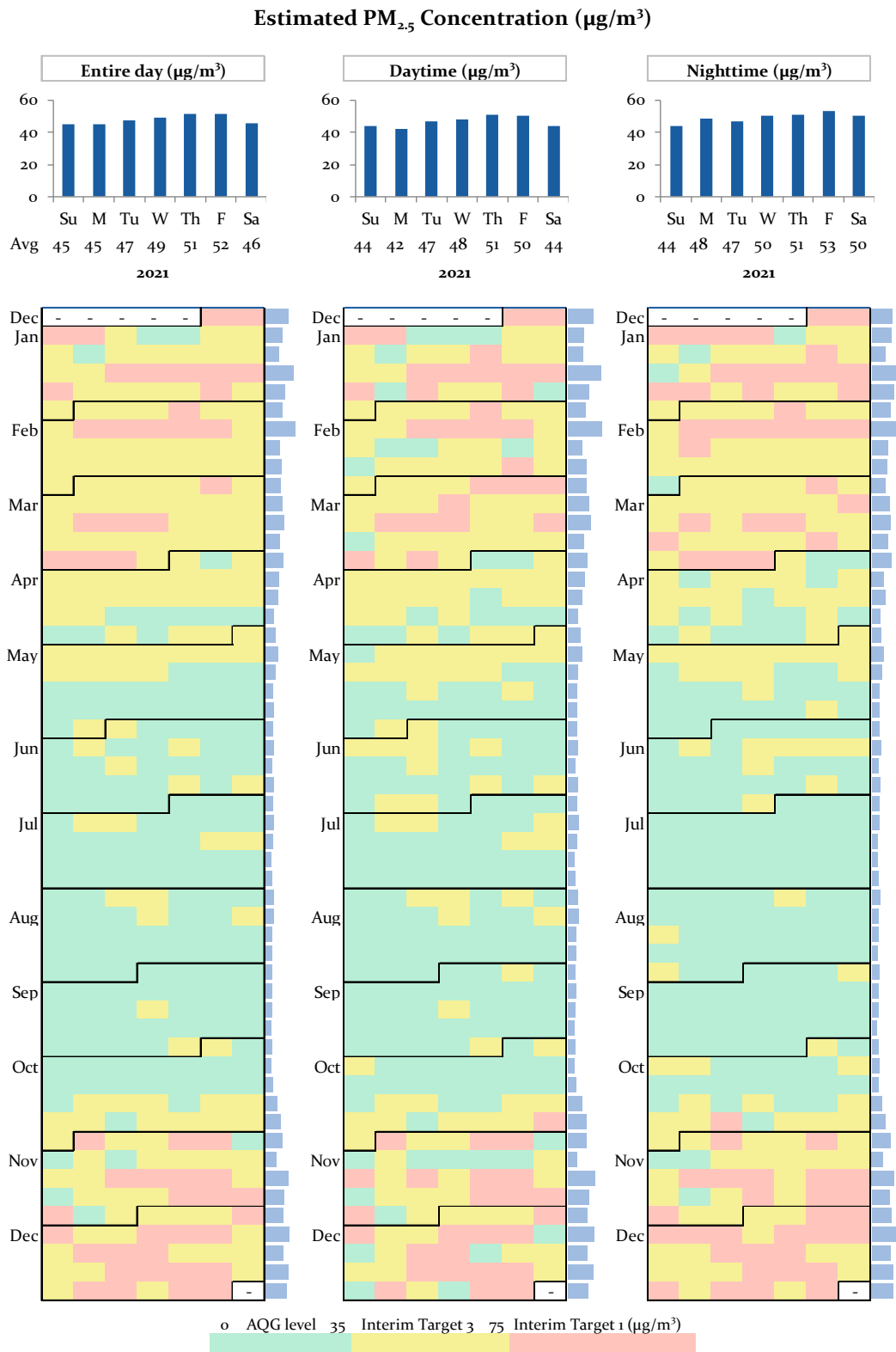


Figure A2. Temporal distribution of the PM_{2.5} concentration across 2021, depicting the daily, weekly, and weekly mean variations in the PM_{2.5} concentration. The breaks and labels of PM_{2.5} concentration adhere to the guidelines established by the Ministry of Ecology and Environment of the People’s Republic of China [54]. The “entire day” corresponds to 00:00 to 23:59; “daytime” spans from 9 a.m. to 6 p.m.; and “nighttime” encompasses the hours from 12 a.m. to 6 a.m. The definitions of daytime and nighttime align with those used for mobile phone data. This chart was created using the Calendar Chart Template from Vertex42.com [55].

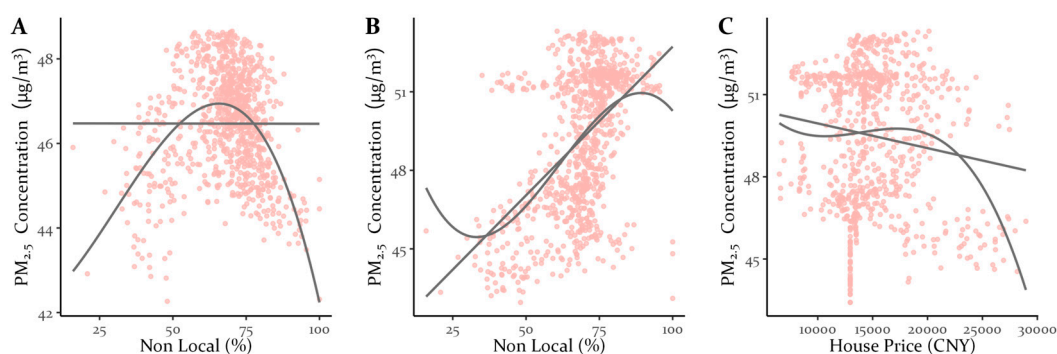


Figure A3. Bivariate relationship between $PM_{2.5}$ concentration and the percentage of nonlocal population and house price. (A) The daytime $PM_{2.5}$ concentration~the percentage of nonlocal. (B) The nighttime $PM_{2.5}$ concentration~the percentage of nonlocal population. (C) The daytime $PM_{2.5}$ concentration~housing price. Smooth lines are fitted using linear regression and polynomial regression, respectively. The “daytime” spans from 9 a.m. to 6 p.m.; and the “nighttime” encompasses the hours from 12 a.m. to 6 a.m.

References

1. Fiordelisi, A.; Piscitelli, P.; Trimarco, B.; Coscioni, E.; Iaccarino, G.; Sorriento, D. The Mechanisms of Air Pollution and Particulate Matter in Cardiovascular Diseases. *Heart Fail. Rev.* **2017**, *22*, 337–347. [[CrossRef](#)]
2. Hamra, G.B.; Guha, N.; Cohen, A.; Laden, F.; Raaschou-Nielsen, O.; Samet, J.M.; Vineis, P.; Forastiere, F.; Saldiva, P.; Yorifuji, T.; et al. Outdoor Particulate Matter Exposure and Lung Cancer: A Systematic Review and Meta-Analysis. *Environ. Health Perspect.* **2014**, *122*, 906–911. [[CrossRef](#)] [[PubMed](#)]
3. Liu, C.; Chen, R.; Sera, F.; Vicedo-Cabrera, A.M.; Guo, Y.; Tong, S.; Coelho, M.S.Z.S.; Saldiva, P.H.N.; Lavigne, E.; Matus, P.; et al. Ambient Particulate Air Pollution and Daily Mortality in 652 Cities. *N. Engl. J. Med.* **2019**, *381*, 705–715. [[CrossRef](#)] [[PubMed](#)]
4. Pui, D.Y.H.; Chen, S.-C.; Zuo, Z. $PM_{2.5}$ in China: Measurements, Sources, Visibility and Health Effects, and Mitigation. *Particuology* **2014**, *13*, 1–26. [[CrossRef](#)]
5. Cao, J.; Xu, H.; Xu, Q.; Chen, B.; Kan, H. Fine Particulate Matter Constituents and Cardiopulmonary Mortality in a Heavily Polluted Chinese City. *Environ. Health Perspect.* **2012**, *120*, 373–378. [[CrossRef](#)]
6. Crouse, D.L.; Peters, P.A.; van Donkelaar, A.; Goldberg, M.S.; Villeneuve, P.J.; Brion, O.; Khan, S.; Atari, D.O.; Jerrett, M.; Pope, C.A.; et al. Risk of Non Accidental and Cardiovascular Mortality in Relation to Long-Term Exposure to Low Concentrations of Fine Particulate Matter: A Canadian National-Level Cohort Study. *Environ. Health Perspect.* **2012**, *120*, 708–714. [[CrossRef](#)]
7. Weuve, J.; Puett, R.C.; Schwartz, J.; Yanosky, J.D.; Laden, F.; Grodstein, F. Exposure to Particulate Air Pollution and Cognitive Decline in Older Women. *Arch. Intern. Med.* **2012**, *172*, 219–227. [[CrossRef](#)] [[PubMed](#)]
8. Braithwaite, I.; Zhang, S.; Kirkbride, J.B.; Osborn, D.P.J.; Hayes, J.F. Air Pollution (Particulate Matter) Exposure and Associations with Depression, Anxiety, Bipolar, Psychosis and Suicide Risk: A Systematic Review and Meta-Analysis. *Environ. Health Perspect.* **2019**, *127*, 126002. [[CrossRef](#)]
9. Asch, P.; Seneca, J.J. Some Evidence on the Distribution of Air Quality. *Land Econ.* **1978**, *54*, 278–297. [[CrossRef](#)]
10. Shan, Z.; Li, H.; Pan, H.; Yuan, M.; Xu, S. Spatial Equity of $PM_{2.5}$ Pollution Exposures in High-Density Metropolitan Areas Based on Remote Sensing, LBS and GIS Data: A Case Study in Wuhan, China. *Int. J. Environ. Res. Public Health* **2022**, *19*, 12671. [[CrossRef](#)]
11. Gouveia, N.; Slovic, A.D.; Kanai, C.M.; Soriano, L. Air Pollution and Environmental Justice in Latin America: Where Are We and How Can We Move Forward? *Curr. Environ. Health Rep.* **2022**, *9*, 152–164. [[CrossRef](#)] [[PubMed](#)]
12. Jerrett, M.; Burnett, R.T.; Kanaroglou, P.; Eyles, J.; Finkelstein, N.; Giovis, C.; Brook, J.R. A GIS—Environmental Justice Analysis of Particulate Air Pollution in Hamilton, Canada. *Environ. Plan. A* **2001**, *33*, 955–973. [[CrossRef](#)]
13. Chakraborty, J. Cancer Risk from Exposure to Hazardous Air Pollutants: Spatial and Social Inequities in Tampa Bay, Florida. *Int. J. Environ. Health Res.* **2012**, *22*, 165–183. [[CrossRef](#)] [[PubMed](#)]
14. Zhou, Q.; Zhang, X.; Chen, J.; Zhang, Y. Do Double-Edged Swords Cut Both Ways? Housing Inequality and Haze Pollution in Chinese Cities. *Sci. Total Environ.* **2020**, *719*, 137404. [[CrossRef](#)] [[PubMed](#)]
15. Abel, T.D.; White, J. Skewed Risks and Gentrified Inequities: Environmental Exposure Disparities in Seattle, Washington. *Am. J. Public Health* **2011**, *101*, S246–S254. [[CrossRef](#)] [[PubMed](#)]
16. Jiang, Y.; Yang, Y. Environmental Justice in Greater Los Angeles: Impacts of Spatial and Ethnic Factors on Residents’ Socioeconomic and Health Status. *Int. J. Environ. Res. Public Health* **2022**, *19*, 5311. [[CrossRef](#)] [[PubMed](#)]
17. Maantay, J. Asthma and Air Pollution in the Bronx: Methodological and Data Considerations in Using GIS for Environmental Justice and Health Research. *Health Place* **2007**, *13*, 32–56. [[CrossRef](#)]

18. Stuart, A.L.; Mudhasakul, S.; Sriwatanapongse, W. The Social Distribution of Neighborhood-Scale Air Pollution and Monitoring Protection. *J. Air Waste Manag. Assoc.* **2009**, *59*, 591–602. [CrossRef] [PubMed]
19. Chakraborty, J.; Green, D. Australia's First National Level Quantitative Environmental Justice Assessment of Industrial Air Pollution. *Environ. Res. Lett.* **2014**, *9*, 044010. [CrossRef]
20. Ghorbani, S.; Salehi, E.; Faryadi, S.; Jafari, H.R. Geospatial Analysis of the Distribution of Air Pollutant Emissions in Tehran with a Focus on Environmental Justice. *Int. J. Ecosyst. Ecol. Sci.* **2020**, *10*, 235–248. [CrossRef]
21. Chaix, B.; Gustafsson, S.; Jerrett, M.; Kristersson, H.; Lithman, T.; Boalt, A.; Merlo, J. Children's Exposure to Nitrogen Dioxide in Sweden: Investigating Environmental Injustice in an Egalitarian Country. *J. Epidemiol. Community Health* **2006**, *60*, 234–241. [CrossRef] [PubMed]
22. Gu, L.; Rosenberg, M.; Zeng, J. The impacts of socioeconomic and environmental factors on self-rated health status among different income groups in China. *Geogr. Res.* **2017**, *36*, 1257–1270. [CrossRef]
23. Chen, X.; Feng, J. Health effects of built environment based on a comparison of walkability and air pollution: A case study of Nanjing City. *Prog. Geogr.* **2019**, *38*, 296–304. [CrossRef]
24. Fotheringham, A.S.; Yue, H.; Li, Z. Examining the Influences of Air Quality in China's Cities Using Multi-scale Geographically Weighted Regression. *Trans. GIS* **2019**, *23*, 1444–1464. [CrossRef]
25. Long, Y.; Wang, J.; Wu, K.; Zhang, J. Population Exposure to Ambient PM2.5 at the Subdistrict Level in China. *Int. J. Environ. Res. Public Health* **2018**, *15*, 2683. [CrossRef] [PubMed]
26. Crols, T.; Malleson, N. Quantifying the Ambient Population Using Hourly Population Footfall Data and an Agent-Based Model of Daily Mobility. *Geoinformatica* **2019**, *23*, 201–220. [CrossRef] [PubMed]
27. Liu, H.; Liu, J.; Li, M.; Gou, P.; Cheng, Y. Assessing the Evolution of PM2.5 and Related Health Impacts Resulting from Air Quality Policies in China. *Environ. Impact Assess. Rev.* **2022**, *93*, 106727. [CrossRef]
28. Zhang, Z.; Wang, J.; Hart, J.E.; Laden, F.; Zhao, C.; Li, T.; Zheng, P.; Li, D.; Ye, Z.; Chen, K. National Scale Spatiotemporal Land-Use Regression Model for PM2.5, PM10 and NO2 Concentration in China. *Atmos. Environ.* **2018**, *192*, 48–54. [CrossRef]
29. Xu, Y.; Wei, M.; Zou, B.; Guo, Z.; Li, S. Spatial-Temporal Variation and Spatial Differentiation Geographic Detection of PM2.5 Concentration in Shandong Province Based on Spatial Scale Effect. *Environ. Sci.* **2023**. *Online First*. [CrossRef]
30. Chen, B.; Song, Y.; Jiang, T.; Chen, Z.; Huang, B.; Xu, B. Real-Time Estimation of Population Exposure to PM2.5 Using Mobile- and Station-Based Big Data. *Int. J. Environ. Res. Public Health* **2018**, *15*, 573. [CrossRef]
31. He, L.; Páez, A.; Liu, D. Built Environment and Violent Crime: An Environmental Audit Approach Using Google Street View. *Comput. Environ. Urban Syst.* **2017**, *66*, 83–95. [CrossRef]
32. He, L.; Páez, A.; Jiao, J.; An, P.; Lu, C.; Mao, W.; Long, D. Ambient Population and Larceny-Theft: A Spatial Analysis Using Mobile Phone Data. *ISPRS Int. J. Geo-Inf.* **2020**, *9*, 342. [CrossRef]
33. Lai, S.; Bogoch, I.I.; Ruktanonchai, N.W.; Watts, A.; Lu, X.; Yang, W.; Yu, H.; Khan, K.; Tatem, A.J. Assessing Spread Risk of COVID-19 in Early 2020. *Data Sci. Manag.* **2022**, *5*, 212–218. [CrossRef]
34. Panigutti, C.; Tizzoni, M.; Bajardi, P.; Smoreda, Z.; Colizza, V. Assessing the Use of Mobile Phone Data to Describe Recurrent Mobility Patterns in Spatial Epidemic Models. *R. Soc. Open Sci.* **2017**, *4*, 160950. [CrossRef] [PubMed]
35. Reades, J.; Calabrese, F.; Ratti, C. Eigenplaces: Analysing Cities Using the Space—Time Structure of the Mobile Phone Network. *Environ. Plann. B* **2009**, *36*, 824–836. [CrossRef]
36. Sun, L.; Zhang, H.; Fang, C. Data Security Governance in the Era of Big Data: Status, Challenges, and Prospects. *Data Sci. Manag.* **2021**, *2*, 41–44. [CrossRef]
37. Abitbol, J.L.; Karsai, M. Interpretable Socioeconomic Status Inference from Aerial Imagery through Urban Patterns. *Nat. Mach. Intell.* **2020**, *2*, 684–692. [CrossRef]
38. Guo, S.; Fang, F.; Zhou, T.; Zhang, W.; Guo, Q.; Zeng, R.; Chen, X.; Liu, J.; Lu, X. Improving Google Flu Trends for COVID-19 Estimates Using Weibo Posts. *Data Sci. Manag.* **2021**, *3*, 13–21. [CrossRef]
39. Llorente, A.; Garcia-Herranz, M.; Cebrian, M.; Moro, E. Social Media Fingerprints of Unemployment. *PLoS ONE* **2015**, *10*, e0128692. [CrossRef] [PubMed]
40. Suel, E.; Bhatt, S.; Brauer, M.; Flaxman, S.; Ezzati, M. Multimodal Deep Learning from Satellite and Street-Level Imagery for Measuring Income, Overcrowding, and Environmental Deprivation in Urban Areas. *Remote Sens. Environ.* **2021**, *257*, 112339. [CrossRef]
41. Wang, L.; He, S.; Su, S.; Li, Y.; Hu, L.; Li, G. Urban Neighborhood Socioeconomic Status (SES) Inference: A Machine Learning Approach Based on Semantic and Sentimental Analysis of Online Housing Advertisements. *Habitat Int.* **2022**, *124*, 102572. [CrossRef]
42. Wei, J.; Li, Z.; Lyapustin, A.; Wang, J.; Dubovik, O.; Schwartz, J.; Sun, L.; Li, C.; Liu, S.; Zhu, T. First Close Insight into Global Daily Gapless 1 Km PM2.5 Pollution, Variability, and Health Impact. *Nat. Commun.* **2023**, *14*, 8349. [CrossRef] [PubMed]
43. Wang, X. Historical Data of Air Quality in China. Available online: <https://quotsoft.net/air/> (accessed on 7 June 2022).
44. He, G.; Pan, Y.; Tanaka, T. The Short-Term Impacts of COVID-19 Lockdown on Urban Air Pollution in China. *Nat. Sustain.* **2020**, *3*, 1005–1011. [CrossRef]
45. Kumari, P.; Toshniwal, D. Impact of Lockdown on Air Quality over Major Cities across the Globe during COVID-19 Pandemic. *Urban Clim.* **2020**, *34*, 100719. [CrossRef] [PubMed]

46. Romanillos, G.; García-Palomares, J.C.; Moya-Gómez, B.; Gutiérrez, J.; Torres, J.; López, M.; Cantú-Ros, O.G.; Herranz, R. The City Turned off: Urban Dynamics during the COVID-19 Pandemic Based on Mobile Phone Data. *Appl. Geogr.* **2021**, *134*, 102524. [[CrossRef](#)] [[PubMed](#)]
47. Chan, K.W.; Zhang, L. The *Hukou* System and Rural-Urban Migration in China: Processes and Changes. *China Q.* **1999**, *160*, 818–855. [[CrossRef](#)] [[PubMed](#)]
48. Coffee, N.T.; Lockwood, T.; Hugo, G.; Paquet, C.; Howard, N.J.; Daniel, M. Relative Residential Property Value as a Socio-Economic Status Indicator for Health Research. *Int. J. Health Geogr.* **2013**, *12*, 22. [[CrossRef](#)] [[PubMed](#)]
49. Tomba, L. *The Government Next Door: Neighborhood Politics in Urban China*; Cornell University Press: Ithaca, NY, USA, 2014.
50. Páez, A.; Farber, S.; Wheeler, D. A Simulation-Based Study of Geographically Weighted Regression as a Method for Investigating Spatially Varying Relationships. *Environ. Plan. A* **2011**, *43*, 2992–3010. [[CrossRef](#)]
51. Lu, B.; Hu, Y.; Yang, D.; Liu, Y.; Liao, L.; Yin, Z.; Xia, T.; Dong, Z.; Harris, P.; Brunsdon, C.; et al. GWmodelS: A Software for Geographically Weighted Models. *SoftwareX* **2023**, *21*, 101291. [[CrossRef](#)]
52. Bivand, R.; Yu, D.; Nakaya, T.; Garcia-Lopez, M.-A. Spgwr: Geographically Weighted Regression. Available online: <https://CRAN.R-project.org/package=spgwr> (accessed on 25 March 2023).
53. World Health Organization. *WHO Global Air Quality Guidelines: Particulate Matter (PM_{2.5} and PM₁₀), Ozone, Nitrogen Dioxide, Sulfur Dioxide and Carbon Monoxide*; World Health Organization: Geneva, Switzerland, 2021; ISBN 978-92-4-003422-8.
54. Ministry of Ecology and Environment of the People's Republic of China. Ambient Air Quality Standards. Available online: https://www.mee.gov.cn/ywgz/fgbz/bz/bzwb/dqjh/bh/dqhzjlbz/201203/t20120302_224165.shtml (accessed on 22 June 2024).
55. Wittwer, J. Calendar Heat Map Template. Available online: <https://www.vertex42.com/ExcelTemplates/calendar-chart.html> (accessed on 12 April 2022).
56. Lu, D.; Xu, J.; Yue, W.; Mao, W.; Yang, D.; Wang, J. Response of PM_{2.5} Pollution to Land Use in China. *J. Clean. Prod.* **2020**, *244*, 118741. [[CrossRef](#)]
57. Ma, J.; Liu, B.; Mitchell, G.; Dong, G. A Spatial Analysis of Air Pollution and Environmental Inequality in Beijing, 2000–2010. *J. Environ. Plan. Manag.* **2019**, *62*, 2437–2458. [[CrossRef](#)]
58. Chen, J.; Chen, S.; Landry, P.F. Migration, Environmental Hazards, and Health Outcomes in China. *Soc. Sci. Med.* **2013**, *80*, 85–95. [[CrossRef](#)] [[PubMed](#)]
59. Xi'an Municipal People's Government Xi An Cheng Shi Zong Ti Gui Hua 2008–2020. Available online: <http://zygh.xa.gov.cn/ywzd/cxghsgsb/ghsgsb/62876060f8fd1c0bdc995ed3.html> (accessed on 26 October 2023).
60. Xi'an Natural Resources and Planning Bureau Xi An Shi Guo Tu Kong Jian Gui Hua 2021–2035 Cao An Gong Shi. Available online: <http://www.xa.gov.cn/index/ttpt/636a2fa2f8fd1c4c21276937.html> (accessed on 3 March 2023).
61. Solinger, D.J. *Contesting Citizenship in Urban China: Peasant Migrants, the State, and the Logic of the Market*; University of California Press: Berkeley, CA, USA, 1999.
62. Somers, M.R.; Gibson, G.D. Reclaiming the Epistemological “Other”: Narrative and the Social Constitution of Identity. In *Social Theory and the Politics of Identity*; Craig, C., Ed.; Blackwell: Oxford, UK; Cambridge, MA, USA, 1994; pp. 37–99.
63. Li, Y.; Zhu, D.; Zhao, J.; Zheng, X.; Zhang, L. Effect of the Housing Purchase Restriction Policy on the Real Estate Market: Evidence from a Typical Suburb of Beijing, China. *Land Use Policy* **2020**, *94*, 104528. [[CrossRef](#)]
64. Liu, Y. Introduction to Land Use and Rural Sustainability in China. *Land Use Policy* **2018**, *74*, 1–4. [[CrossRef](#)]
65. Yu, Q.; Hui, E.C.-M.; Shen, J. Do Local Governments Capitalise on the Spillover Effect in the Housing Market? Quasi-Experimental Evidence from House Purchase Restrictions in China. *Land Use Policy* **2023**, *133*, 106851. [[CrossRef](#)]
66. The People's Bank of China. Notice of the People's Bank of China on Adjusting the Policy on Personal Housing Loans. Available online: <http://www.pbc.gov.cn/goutongjiaoliu/113456/113469/3014377/index.html> (accessed on 28 February 2024).
67. The People's Government of Beijing. Municipality Notice on Adjusting and Optimizing the Standards for Ordinary Housing and Personal Housing Loan Policies in Beijing. Available online: https://www.beijing.gov.cn/zhengce/zhengcefaui/202312/t20231214_3500672.html (accessed on 28 February 2024).

Disclaimer/Publisher's Note: The statements, opinions and data contained in all publications are solely those of the individual author(s) and contributor(s) and not of MDPI and/or the editor(s). MDPI and/or the editor(s) disclaim responsibility for any injury to people or property resulting from any ideas, methods, instructions or products referred to in the content.